

## DESIGN METHOD TO COUNTER THE ABRASION OF HYDRAULIC STRUCTURES DUE TO ICE SHEET MOVEMENTS

Fumihoro, Hara.<sup>1</sup>, Kaori, Ohshima.<sup>2</sup>, Masakuni, Hanada.<sup>3</sup>,  
Masuyuki, Ujihira.<sup>4</sup>, Harukuni, Tachibana.<sup>4</sup>, Hiroshi, Saeki.<sup>5</sup>

### ABSTRACT

We have been systematically studying the abrasion of structures (e.g. bridge piers and intake towers) caused by the movement of ice sheets in rivers. From the results of our past studies, we found that the three factors of contact pressure of the ice sheet acting on the surface of a bridge pier, concentration and median diameter of solid particles contained in ice sheets and properties of materials strongly affect the abrasion rate.

In this study, we summarize the results of our fundamental studies and give a method to estimate the abrasion depth. From experimental results and the results of surveys on rivers, etc., in Hokkaido, we also give a method to determine the necessary design constants.

### 1 Introduction

In some regions, including North America, Russia and China, where snow melts in early spring beginning at the upper streams of rivers, problems exist such as floods caused by ice jams and various ice forces that act on the superstructures of bridges or bridge piers that often greatly damage them.

The ice of frozen rivers in Japan does not cause much damage to bridges compared with other cold-climate countries because of the much higher altitude of upper streams than for lower streams and the generally lower temperatures at the level of upper streams. As a result, ice begins to melt at the lower levels of streams. However, some bridges and piers spanning the rivers in northern Hokkaido, especially over the river mouths along the Okhotsk Sea, have been repaired because of abrasion, supposedly due to the action of ice. However, little is known about the damage or its mechanism. Piers have to be repaired in a working environment that is invariably affected by river water and that has to avoid obstructing traffic on the bridge. Ensuring the safety of the working environment and setting various restrictions in the work space during the working period make the work costly. Thus, if the amount of abrasion caused by ice

1.Senior Researer, Hokkaidou Development Engineering Center, 011, South-1, East-2, Chuo-ku, Sapporo, Hokkaido, Japan

2.Graduate Student, Faculty of Engineering, Hokkaido University, 066, North-13, West-8, Kita-ku, Sapporo, Japan

3.Engineer, KAJIMA Corporation, 006, North-3, West-3, chuo-ku, Sapporo, Hokkaido, Japan

4.Assistant Professor, Faculty of Engineering, Hokkaido University

5.Professor, Faculty of Engineering, Hokkaido University

movement can be estimated and taken into consideration at the time of the bridge design, this will help to reduce the cost of future maintenance.

## 2 The basic concept of the abrasion test on the surface of concrete structures by ice movements

The interactions between the edge of the ice sheet and the surface of the structure when ice forces caused by the moving ice sheets act on concrete structures, especially the destruction mechanism of the ice sheet and the actions of the ice forces, is important to understand. Frictional forces between the ice sheet and the structure should be focused upon, especially in terms of the abrasion of the material of the structure. These frictional forces are equal to the contact pressures (stresses acting on the structure in the normal direction) multiplied by the coefficient of friction between the ice sheet and the surface of the structure. Also, for the development of test devices, contact pressures should be considered. Moreover, to understand the ice forces acting on the structure, the strain velocity and the aspect ratio at the time of ice sheet intrusion must be carefully considered. According to Michel et al. (1977), the strain velocity at the time of ice sheet intrusion can be represented by the following equation:

$$\varepsilon p = V/4W$$

where  $V$  represents the intrusion velocity of the ice sheet and  $W$  represents the width of the structure.

When  $\varepsilon p$  is small, the ice sheet is ductily destroyed, and when  $\varepsilon p$  is large, the ice sheet is brittly destroyed. Also, near the transitional zone where  $\varepsilon p \approx 10^{-3} \text{sec}^{-1}$ , the ice forces are large and the period of destruction is also large. Where  $\varepsilon p > 10^{-3} \text{sec}^{-1}$ , the changes in ice forces clearly show that the relative velocity sometimes falls to zero at the contact point of the structure and ice sheet. Thus, between the ice sheet and the surface of the structure, kinetic friction and static friction act alternately. The coefficient of static friction is approximately twice as large as the coefficient of kinetic friction (Saeki et al. 1984). Thus, the frictional forces of static friction are also larger.

In addition, factors affecting frictional stress are the contact pressure, the ice sheet strength, and the relative velocity (Saeki et al. 1984). To summarize, a test device to measure the abrasion of the concrete surface by ice movements must fulfill the following conditions.

- (1) The test device must permit changes in the contact pressure, the ice sheet temperature and the relative velocity.
- (2) Static and kinetic friction must act during the test.
- (3) The amount of abrasion must be measured easily and accurately.
- (4) Although the concrete specimen used in the test is exposed to frictional forces and pressed onto an ice sheet with a certain pressure for a long time, the ice sheet should not be melted by the frictional heat.
- (5) At the contact point, shavings of the ice sheet and concrete are produced, but they must be

- removed by a suitable method.
- (6) The coefficient of friction between the concrete and ice sheet must remain constant both in water and in the air.
  - (7) The results gained must be useful to predict the actual amount of abrasion and to evaluate measures to prevent abrasion.

The test device suitable for these conditions was developed by Saeki et al (1984). from various tests on the coefficient of friction of materials, including ice sheets (Fig.1). Fig.2 concept of the method. In the test, sea ice of width 8cm, length 70cm, and thickness 8-12 cm reciprocates horizontally, and a trapezoidal concrete specimen is pressed onto the sea ice by vertical stresses. The relative velocity is determined by the coefficient of friction test, and the sea ice reciprocates at 2cm/s, 5cm/s, and 20cm/s. Thus, static and kinetic frictions act alternately. Also, because in this test the device is kept in a room where low temperatures must be maintained, the range of temperatures is very wide. The range of the contact pressures is 0-70MPa. In addition, the width of the concrete specimen is 10cm. Thus the width of abrasion is 8cm, leaving 1cm from each edge unabraded. Therefore, measurement of the depth of abrasion is feasible by comparing each edge and the area within the range of abrasion. Consequently, it can be measured accurately. Also, an air compressor sends cold air to the contact point between the concrete specimen and the two sides of the sea ice to remove concrete and ice shavings and to cool down the surface of the ice. This test device has fewer disadvantages than the other devices. The only disadvantage is that the ice can be broken due to fatigue from the movement of the concrete specimen on the ice at high contact pressures (more than or equal to 1.5MPa), so frequent replacement of the ice is required.

Currently, a total of seven types of abrasion test equipment have been developed in the world, including the one developed by Saeki et al. We investigated the characteristics of each test equipment and evaluated its benefits and defects and clarified that the most reasonable abrasion test equipment in terms of reproducing the abrasion by ice movement was this sliding abrasion test.

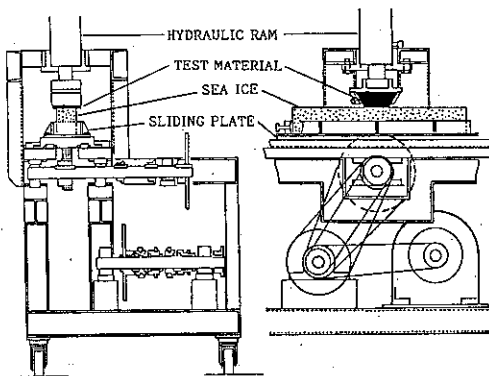


Fig. 1. Sliding abrasion test (Saeki).

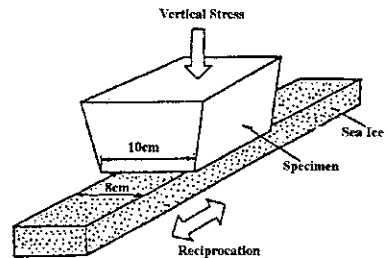


Fig. 2. The basic concept of sliding abrasion test.

### 3 Experimental Results

In this study, we used five types of concrete as specimens: normal concrete (N.C.) containing ordinary coarse and fine aggregates and with unconfined compressive strength ( $\sigma_c$ ) of 568 kgf/cm<sup>2</sup>; high-strength light-weight concrete (L.W.C.) containing ordinary fine and light-weight coarse aggregates with the same unconfined compressive strength; high-strength light-weight concrete (L.L.W.C.) containing both light-weight fine and coarse aggregates with the same unconfined compressive strength; and light-weight concrete (L.W.C.) with unconfined compressive strength of 350 kgf/cm<sup>2</sup> and 700 kgf/cm<sup>2</sup> and various coating materials such as paint, synthetic materials, steel and rocks. The maximum size of aggregates in the concrete specimen was 25mm. The mix proportions of the aggregates in these five types of concrete are described in Saeki et al. (1985).

#### 3.1 Relationship between the mean abrasion amount and the sliding distance

The characteristics of abrasion of concrete ought to change with the advance of the abrasion from the surface, because concrete is a mixture of cement paste and coarse and fine aggregates. Fig.3 shows the relationship between the mean abrasion amount and the sliding distance (L) for fresh water ice. These are the results of the experiment made under fixed conditions where the ice temperature was -10°C, the vertical stress was 10kgf/cm<sup>2</sup> and the relative velocity was 5 cm/sect using four types of concrete, i.e., N.C., L.W.C. and L.L.W.C. with unconfined compressive strength of 568kgf/cm<sup>2</sup> and L.W.C. with unconfined compressive strength of 350kgf/cm<sup>2</sup>. The figure shows that the process of change of the mean abrasion amount according to the sliding distance (L) can be divided into three main stages. Regardless of the differences in the aggregates and the unconfined compressive strength of the concrete, the same process of change was observed in all the types of concrete.

- (1) When the sliding distance (L) was less than 3km and the mean abrasion amount was less than 0.25mm from the concrete surface, the mean abrasion rate of 0.085mm/km was rather large, because the uneven concrete surface and cement paste in the surface layer were abraded. At this stage, the aggregate could hardly be seen on the surface of the specimens after the abrasion test. We named this range (within 0.25mm of the concrete surface) the surface region.
- (2) When the sliding distance was between 3km and 11km and the mean abrasion amount was between 0.25mm and 0.61mm, the mean abrasion rate was smaller than for the surface region, an average of 0.044mm/km. In this range, part of the coarse and fine aggregates were exposed on the surface of the concrete; this range was named the transition region.
- (3) When the sliding distance was more than 11km, the mean abrasion rate decreased further to approx. 0.012mm/km, which was about one seventh of the surface layer mean abrasion rate. In this range, which was named the stable region, a much more coarse aggregate was exposed.

As the sliding distance reached 11km and the mean abrasion amount reached about 0.61mm from the surface in this experiment, questions remained concerning the continuation of this tendency. Therefore, we made an abrasion test using concrete specimens with completely exposed coarse aggregate, which was made by cutting the surfaces about 6mm-10mm (the area of

exposed coarse aggregate, which was made by cutting the surfaces about 6mm-10mm (the area of the aggregate was 45-60% of the exposed area). Fig.4 shows the results of the test. The conditions of this experiment were the same as for Fig.3, and the three types of concrete, the two containing different aggregates with the same unconfined compressive strength of 568kgf/cm<sup>2</sup> and the other one with unconfined compressive strengths of 350kgf/cm<sup>2</sup>, were used. The relationship between the mean abrasion amount and the sliding distance approximated a straight line, and the mean abrasion rate was 0.012mm/km. This indicates that under the same test conditions, when the mean abrasion amount exceeded about 0.61mm from the concrete surface, the mean abrasion rate was constant, regardless of the strength of concrete and kind of aggregate contained in concrete. As a result, we found that by cutting off the surface layer (6-10mm) of concrete specimens it was possible to shorten the test time considerably, and we used this method in all the later experiments.

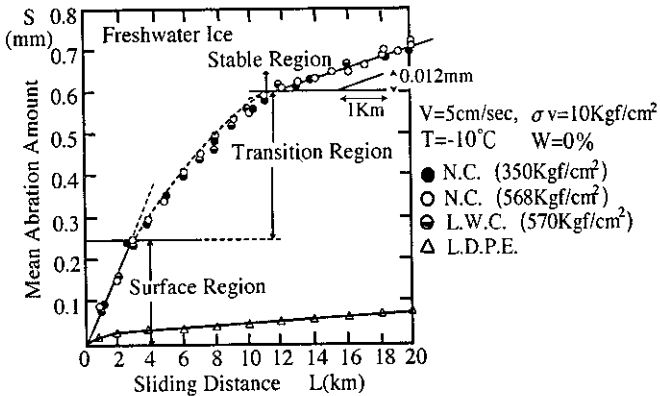


Fig. 3. Abrasion characteristics of various three of concrete according to sliding distance

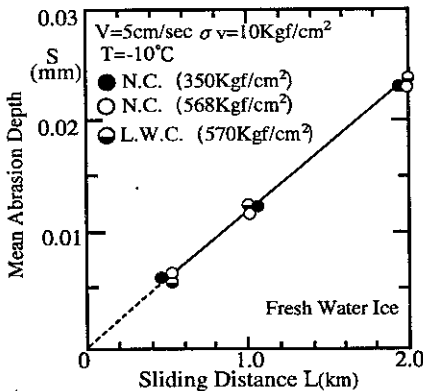


Fig. 4. Relationship between sliding distance and mean abrasion amount (fresh water ice).

### 3.2 Relationship between the relative velocity and the mean abrasion amount

The mean abrasion amount of concrete is dependent on the friction force between sea ice and concrete surfaces. The friction force is shown in general by the product of the vertical direction stress and the coefficient between sea ice and concrete surfaces. The results of past experiments by Saeki et al. (1984) made clear that the coefficients of both kinetic and static friction depend not on the contact area and the contact pressure in a vertical direction, but greatly depend on the roughness of material surfaces and the relative velocity between sea ice and materials. Also, the ice temperature, which is closely related to the strength of sea ice, has different degrees of influence on the friction coefficient according to the kind of material.

According to the results for concrete by Saeki et al (1984), the friction coefficient was influenced by the relative velocity. In the range where the relative velocity ( $V$ ) was higher than 20cm/sec, the friction coefficient did not greatly depend on the relative velocity, while in the range where  $V$  was lower than 20 cm/sec, the friction coefficient rapidly increased as the relative velocity decreased. This characteristic was also found with uncoated steel and with coated steel.

Fig.5 shows the relationship between the relative velocity and the mean abrasion rate for four types of concrete with different unconfined compressive strengths. The experiment was limited because the range of the relative velocity was within 20cm/sec and the quantity of test data was small. However, the experiment showed that as the relative velocity decreased, the mean abrasion rate increased and the degree of the increase in the mean abrasion rate became steeper. This tendency was very similar to the change of the friction coefficient obtained by Saeki et al (1984). As the relative velocity decreased, the mean abrasion rate increased, but on the other hand, the sliding distance ( $L$ ) did not increase much. Accordingly, setting the relative velocity ( $V$ ) at about 5cm/sec to practically examine the characteristics of concrete abrasion is appropriate. Also, if the experiment is made using the relative velocity of about 20cm/sec, the total test time can be reduced. However, renewing sea ice is troublesome, and because the abrasion tester is an alternating motion type, the tester becomes overloaded and vibrates excessively when reversing direction. Therefore, we set 5cm/sec as the standard relative velocity ( $V$ ) for later experiments.

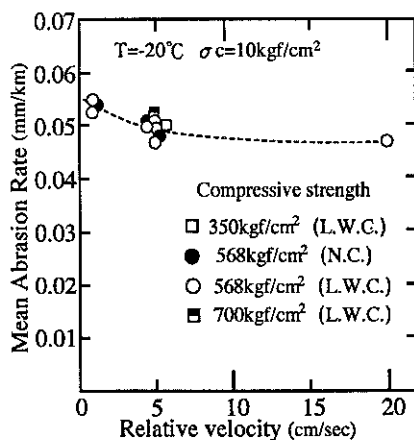


Fig. 5. Relationship between relative velocity and mean abrasion rate (sea ice).

### 3.3 Relationship between the ice temperature and the mean abrasion rate

The friction coefficient between sea ice and certain materials depends on the ice temperature. Fig.6 shows the relationship between the ice temperature and the mean abrasion rate for three types of concrete, each with an unconfined compressive strength of 568kgf/cm<sup>2</sup> and each containing different aggregates. Regardless of the difference in the aggregates of concrete, Fig.6 shows the same change. When the ice temperature (T) was higher than -10°C, the change in the mean abrasion rate against the decline in the ice temperature was small, while the mean abrasion rate rapidly increased when T was lower than -10°C.

Fig.7 shows the relationship between the mean abrasion rate and the contact pressure at different ice temperatures for fresh water ice. In the range where the ice temperature was higher than -10°C. The main factors that influence the mean abrasion rate for fresh water ice are shown by the ice temperature and the contact pressure in Fig. 8.

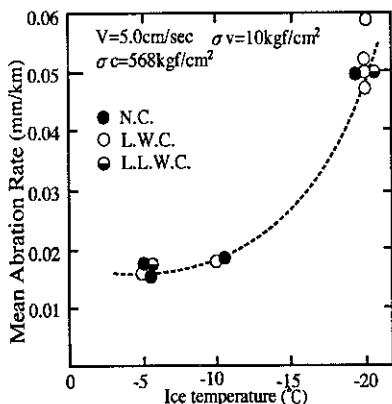


Fig. 6. Relationship between ice temperature and mean abrasion rate (sea ice).

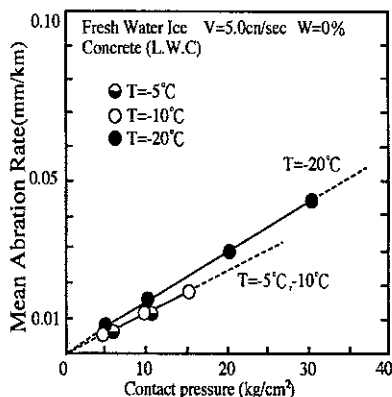


Fig. 7 Relationship between mean and and contact pressure at several ice temperature

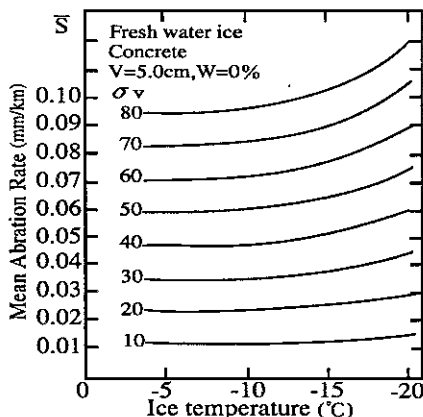


Fig. 8. Estimation of mean abrasion rate.

### 3.4 Relationship between sand concentration, diameter and abrasion rate

When ice contains solid substances, the mean abrasion rate is expected to accelerate in much the same way as when the salt in brine separates out at temperatures of sea ice  $-8^{\circ}\text{C}$  or below. Therefore, the abrasion of concrete caused by fresh water ice containing sand particles is now described.

Fig.9 relationship between the mean abrasion rate ( $\bar{S}$ ) and the contact pressure ( $\sigma v$ ) of our experiment for each median diameter ( $\bar{d}$ ) of particle. In this figure, the concentration of sand particles ( $W$ ) was 0.4%, the ice temperature was  $-10^{\circ}\text{C}$  and the velocity of the ice movement ( $V$ ) was 5cm/sec. The median diameters of the sand particles used were 0.03mm, 0.14mm and 0.7mm. The fresh water ice containing sand had a larger mean abrasion rate compared with the fresh water ice without sand.

When the ice contained much sand of the same median diameter the mean abrasion rate accelerated in a straight line as the contact pressure ( $\sigma v$ ) increased. At the same contact pressure, fresh water ice containing sand of greater median diameter had a higher mean abrasion rate. Fig.10 shows the relationship between each median diameter ( $\bar{d}$ ) and the value  $\bar{S}d/\bar{S}(W=0)$ , which is the dimensionless state when the mean abrasion rate of each median diameter ( $\bar{d}(\bar{S}d)$ ) is divided by the mean abrasion rate without sand ( $\bar{S}(W=0)$ ) with 0.4% as the concentration of the sand ( $W$ ) in ice.

Fig.11 shows the relationship between the sand concentration and the dimensionless value  $\bar{S}w/\bar{S}(W=0)$ , when the mean abrasion rate ( $\bar{S}w$ ), at the ice temperature ( $T$ ) of  $-10^{\circ}\text{C}$  and with the median diameter ( $\bar{d}$ ) and the sand concentration ( $W$ ), is divided by the mean abrasion rate without sand ( $\bar{S}(W=0)$ ). As the figure clearly shows, if the median diameter is the same, the dimensionless mean abrasion rate accelerated with the rise in sand concentration. And if the sand concentration is the same, the mean abrasion rate accelerated with the increase in median diameter (Fig.8). Consequently, the mean abrasion rate, which is the most important parameter to estimate the mean abrasion amount of concrete caused by ice sheet movements, is determined by ice temperature, contact pressure ( $\sigma v$ ) on the surface of concrete, median diameter ( $\bar{d}$ ) of sand particles contained in the ice and sand concentration ( $W$ ).

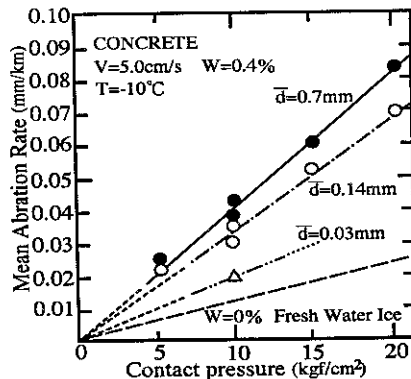


Fig. 9. Relationship between mean abrasion rate, contact pressure and median diameter.



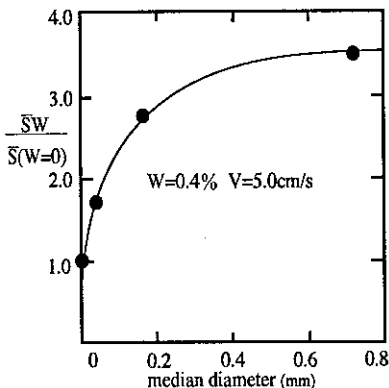


Fig. 10. Median diameter and dimensionless mean abrasion rate.

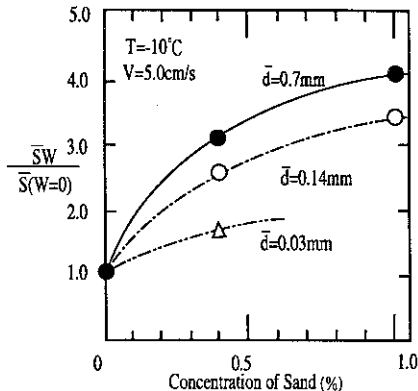


Fig. 11. Relationship between sand concentration, diameter and dimensionless mean abrasion rate.

#### 4 Method of estimating the amount of abrasion on the surface of piers due to movement of ice floes

We have been making basic experiments for twelve years on various materials concerning the properties of abrasion from the movements of sea and freshwater ice, and the fact has become evident that if the contact pressure between ice floes and the structure, and the central grain diameter and the concentration of sand in the floes are known, the abrasion rate on the concrete pier can be determined.

When the abrasion rate on the concrete is known, the distribution of abrasion on the pier can be found from changes in the traveling distances of floes and the water levels when the floes move. Fig. 12 is a flow chart to estimate the amount of abrasion.

From results of fundamental studies mentioned above, we propose the following equation to estimate the abrasion depth:

$$S = a \times K \times \sigma v \times L \times N \quad (-10^\circ\text{C} \leq T \leq 0^\circ\text{C})$$

where

$S$  = abrasion depth of a hydraulic structure (mm)

$a$  = abrasion rate of each material (mm/km)/(kgf/cm<sup>2</sup>)

$\sigma v$  = contact pressure of an ice sheet acting on a structure (kgf/cm<sup>2</sup>)

$K$  = dimensionless abrasion rate

(abrasion rate of ice sheet containing solid particles / abrasion rate of ice sheet not containing solid particles)

$L$  = yearly average of the sliding distance of an ice sheet (km)

$N$  = life period of a bridge pier (km/years)

$T$  = ice temperature (°C)

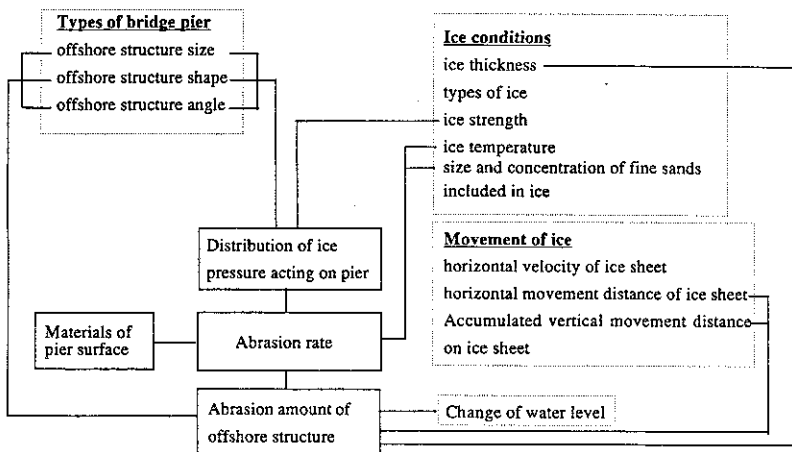


Fig. 12. Flow chart for estimating abrasion depth.

#### 4.1 Abrasion rate of each material

We made experiments on concrete, steel, synthetic materials and stone with a sliding-type abrasion apparatus, and clarified the abrasion rate (mm/km) of each material and abrasion properties of various materials. Table.1 summarizes the abrasion rate versus unit contact each pressure. The abrasion rate due to sea ice is larger than that due to fresh water ice. It is main reason that the surface of sea ice is not smooth because of the existence of brine pockets.

Table. 1 Abrasion rates of various materials

T=-10°C		
material	abrasion rate of sea ice (mm/kg)/(kgf/cm <sup>2</sup> )	abrasion rate of fresh water ice (mm/kg)/(kgf/cm <sup>2</sup> )
concrete	0.00178	0.00120
steel	0.00030	0.00027
LDPE	0.00022	0.00025
sand stone	0.00049	0.00029
tuff	0.00251	0.00589
pyroxene andesite	0.00084	0.00037
dacite A	0.00065	0.00100
dacite B	0.00177	0.00277

#### 4.2 Contact pressure

The maximum contact pressure ( $\sigma_v$ ) on the surface of structures due to an ice sheet depends on the unconfined compressive strength ( $\sigma_c$ ) of the ice sheet. Table.2 summarizes the theoretical equations and experimental equations proposed for the relationship between the unconfined compressive strength of the ice sheet and the contact pressure.

From the results of research on the distribution of ice pressure acting on an upright structure with a rectangular section by Tanaka et al.(1987) and the research on a structure with a circular section by Saeki et al.(1981), the distribution of ice pressure is influenced by the strain rate which accompanies the aspect ratio and intrusion, and the maximum ice pressure (contact pressure) is about four to five times the uniaxial compressive strength.

We obtained the result that the design contact pressure should be  $4.5 \sigma_c$ .

From results of unconfined compression tests with ice sheets from rivers, lakes and marshes in Hokkaido, we clarified the unconfined compressive strength of ice sheets used for designs (Table.3).

Table 2. Formulas to calculate contact pressures with various cross sectional shapes.

Shape of bridge pier	$\bar{\sigma}_v$	w/h	$\epsilon$	
	$\bar{\sigma}_v = (1.4 + 0.97h/w) \sigma_c$			Theol. formula (Reinicke)
Upright rectangular	$\bar{\sigma}_v = (1 + 0.304h/w) \sigma_c$ $\bar{\sigma}_v = (0.43 - 0.48) \sigma_c$	4 - 5	$10^{-3}$	Theol. formula (Morgenstern, Nattal)
Upright wedge-shape	$\bar{\sigma}_v = 0.25 \sigma_c, a=45$	4 - 5	$10^{-3}$	Exp. formula (Saeki et al.)
Upright circle	$\bar{\sigma}_v = (0.32 - 0.35) \sigma_c$ $\bar{\sigma}_v = (0.83 - 0.91) \sigma_c$	4 - 5	$10^{-3}$	Exp. formula (Saeki) Exp. formula (Saeki)
Inclined circle	$\bar{\sigma}_v = (0.31 - 0.35) \sigma_c$	4 - 5	$10^{-3}$	Exp. formula (Hirayama)

Table 3 Uniaxial compressive strength of ice sheet

	ice temperature	uniaxial compressive strength (kgf/cm <sup>2</sup> )		
		Max	Min	median diameter
Teshio river 1992	-2	75	5	40
	-10	115	25	70
Teshio river 1993	-2	55	5	30
	-10	70	15	42.5
Katsurazawa Lake	-3	50	20	35
	-10	70	45	57.5

### 4.3 Solid particles contained in ice sheets

From the analysis of ice sheets sampled from rivers, lakes and marshes in Hokkaido (Table.4), we found that the maximum concentration of solid particles in ice sheets was 450 mg/l and the maximum median diameter was 250  $\mu$  m (Fig.15). From these results and the results of abrasion experiments made while changing the concentration and median diameter of solid particles, we found that the value of K, the dimensionless abrasion rate, was approximately 1.5 at maximum in Hokkaido.

Table. 4 Concentration and median diameter in ice sheet

area	location	amount of solid particle	median diameter
river	Teshio River	433.9 mg/l	134.3 $\mu$ m
	Rekihune River	17.6 mg/l	20.9 $\mu$ m
lake	Utonai Lake	145.0 mg/l	24.0 $\mu$ m
	Barato Lake	418.0 mg/l	203.1 $\mu$ m
	Syuuparo Lake	64.6 mg/l	12.0 $\mu$ m
	Oikamanae Swamp	27.7 mg/l	15.0 $\mu$ m
	Shinotsu Lake	7.3 mg/l	38.8 $\mu$ m
	Abashiri Lake	75.9 mg/l	153.9 $\mu$ m
	Notori Lake	12.5 mg/l	8.0 $\mu$ m
	Saroma Lake	95.5 mg/l	21.0 $\mu$ m
	Harutori Lake	12.5 mg/l	8.0 $\mu$ m

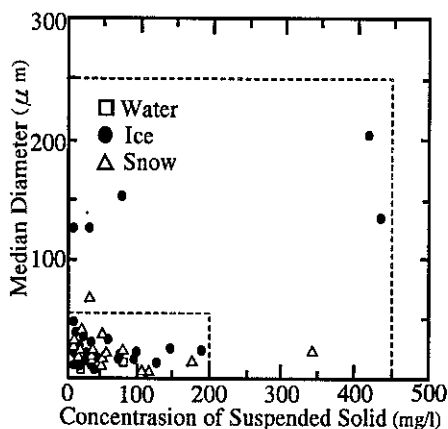


Fig.13 Relationship between concentration of suspended solid and median diameter

## 5 Measures to prevent abrasion of bridge piers

Fig. 14 shows measures to prevent the abrasion of bridge piers due to ice movement from the current evaluation of damage to bridge piers and examples of their repair methods. The measures can be divided into three major categories.

- (1) Thickening the cover to as much as the estimated amount of abrasion for the service life of the bridge so as to maintain structural soundness.
- (2) Coating the upstream side of bridge piers in the ice floe contact area with an abrasion-resistant material that has a stronger resistance against abrasion than the original concrete of pier. As a coating material, steel plate, stone facing, and synthetic materials can be considered.
- (3) The amount of abrasion can be reduced by changing the shape and inclination of the nose. The first method enlarges the cross section, as well as the weight of bridge pier, which results in an increase in horizontal force at the time of an earthquake, as well as in the vertical force and ice force. Because these forces are disadvantageous to the stability of piers, considering them at the time of repair is necessary.

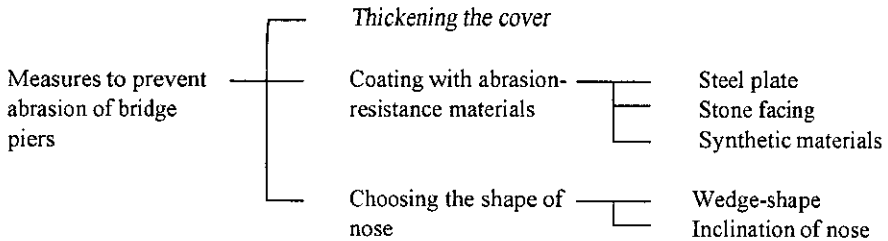


Fig. 14. Measures to prevent the abrasion of bridge piers.

The second method is to coat the concrete surface with abrasion-resistant materials. Table I shows the result of experiments on the abrasion rates between fresh water ice and various materials. The abrasion rates of steel and low-density polyethylene or polyurethane are 1/10 and 1/15 of that of concrete, respectively. Synthetic materials are superior to other materials in terms of abrasion. However, polyethylene cannot stick to concrete directly, and thus, it is necessary to stick it to a steel plate and then put the plate on the concrete. Urethane can be applied to concrete directly, and its thickness can be changed easily. Polyester is not appropriate as a coating material, because smoothing its surface is difficult. In addition, it peels easily.

Before the use of synthetic materials, the influence of deterioration due to ultraviolet radiation, etc., should be determined through outdoor exposure and other tests. Sometimes when ice contains a lot of sand particles, the abrasion rate of synthetic materials is larger than that of concrete: this also needs to be considered. From these points of view, steel or stainless steel, which have already been used abroad, are reliable materials that are easy to apply. They are the best coating materials up to now.

The third method tries to reduce the amount of abrasion by changing the shape of the pier to

decrease the ice force. Table.2 shows the mean contact pressures with various cross sectional shapes.

As a result of our study, we conclude that coating with stainless steel is the best method with the current level of engineering and a wedge-shape cross section is the most effective to reduce the ice force.

## REFERENCES

1. Michel,B. (1979) Ice Mechanics, Quebec, P.Q., Les presses de l'Univer site Laval.
2. Saeki,H., Ono,T., Nakazawa,N., Sakai,M. and Tanaka,S. (1984) The Coefficient of Friction between Sea Ice and Various Materials Used in Offshore Structure. Proc.of Offshore Technology Conference, Vol.1, pp.375-82.
3. Saeki,H., Asai,Y., Izumi and Takeuchi,T. (1985) Study on Abrasion of Concrete due to Sea ice.The 10th Marine Development Symposium, pp.68-73.
4. Tachibana,H., Mizuno,K., Yamashita,T. and Saeki,H., (1991) Characteristics of Suspended Solids in Sea and Lake Ice. Proc. of the 6th International Symposium on Okhotsk Sea & Sea Ice,pp.102-6.
5. Tanaka, Ono and Saeki (1987) The Distribution of Ice Pressure Acting on Offshore Pile Structure and Failure Mechanics of Ice Sheet. Jour. of Offshore Mechanics and Arctic Engineering, Vol.1 pp.76-83,(ASME).
6. Saeki,Ono, Yamada and Ozaki (1981) Study on Force of Sea Ice Acting on Vertical Structures, Proc. of the 28th Japanese Conference on Coastal Engineering, pp.396-400.